Effects of Thickness Extension Mode Resonance Oscillation of Acoustic Waves on Catalytic and Surface Properties. III. Ethanol Decomposition on a Thin Ag Film Catalyst Deposited on Negatively Polarized *z*-cut $LiNbO_3$

N. Saito, Y. Yukawa, and Y. Inoue*

Department of Chemistry, Nagaoka University of Technology, Nagaoka 940-2188, Japan

Received: May 9, 2002

The effects of thickness extension mode resonance oscillation (TERO) of bulk acoustic waves on ethanol decomposition over a 100 nm Ag film deposited on a negatively polarized *z*-cut $LiNbO_3$ crystal ((−)Ag) were studied, and the results were compared with those obtained previously for Ag deposited on a positively polarized *z*-cut $LiNbO_3$ crystal ((+)Ag). In ethylene and acetaldehyde production, the TERO for (−)Ag increased the selective for ethylene production, but the TERO effects on activity and selectivity enhancement were smaller compared to those for (+)Ag. Laser Doppler measurements showed that lattice displacements caused by the TERO were similar between (−)Ag and (+)Ag. In photoelectron emission spectra of (−)Ag, the TERO caused the positive shifts of the threshold energy for electron emission associated with the work function of the Ag surface. The work function increases were considerably smaller for (−)Ag than for (+)Ag, which is considered to be responsible for differences in the catalyst activation between (−)Ag and (+)Ag. A mechanism of different TERO effects between (−)Ag and (+)Ag is discussed.

Introduction

In a series of studies of acoustic waves effects on metal catalysts, the resonance oscillation of bulk acoustic waves generated on poled ferroelectric crystals has proved to be useful not only for catalyst activation but also for the control of reaction paths.[1−11] Recently, we have demonstrated that the effects of resonance oscillation strongly depend on the direction of spontaneous polarization of ferroelectric crystals as a substrate.[12] For a ferroelectric *z*-cut $LiNbO_3$ single crystal with the polarization axis perpendicular to the surface, the thickness extension mode resonance oscillation (TERO) characteristic of lattice displacement vertical to the surface is generated. On the other hand, in the case that an *x*-cut $LiNbO_3$ crystal with a spontaneous polarization axis parallel to the surface is used, the thickness shear mode resonance oscillation (TSRO) characteristic of lattice displacement parallel to the surface is produced. For ethanol decomposition over a thin Ag film catalyst deposited on the two crystals, the TERO caused remarkable increases in the catalytic activity, whereas the TSRO failed to increase the activity. These results indicate that not only kinds of the lattice displacement but also the effects of polarization direction are involved in the acoustic wave effects on catalyst activation.

The polarization axis vertical to the surface means that the crystal exposes a positively polarized surface at one plane and a negatively polarized surface at the opposite plane. In previous studies, thin Ag and Pd films were deposited on a positively polarized surface, while the opposite negative plane was used as an electrode by covering it with a catalytically inactive Au film (the catalyst is referred to as (+)Ag and (+)Pd, respectively).[13,14] The characteristic TERO effects on (+)Ag and (+)Pd have shown that it is of particular importance to elucidate the TERO effects on a metal catalyst combined with a negatively polarized surface.

Thus, in the present work, to obtain information on the role of the polarized surface in the TERO-induced catalyst activation, the TERO effects on a thin Ag film catalyst deposited on a negatively polarized *z*-cut $LiNbO_3$ surface (denoted here as (−)Ag) were studied in detail and were compared with the previous results obtained for (+)Ag. For the characterization of surface lattice movement of (−)Ag catalyst, a 3-D laser Doppler method was employed. Furthermore, photoelectron emission spectra were obtained to clarify the TERO effects on the electronic structures of (−)Ag.

Experimental Sections

The catalyst fabrication was nearly the same as that employed in a previous study of (+)Ag.[13] A single crystal of *z*-cut $LiNbO_3$ (referred to as *z*-LN) 1 mm thick was cut in the shape of 14 mm in width and 44 mm in length. A 100 nm Ag thin film (which worked as an electrode and a catalyst) was deposited by the resistance heating of pure Ag metal in a vacuum on a negatively polarized plane of *z*-LN, and a catalytically inactive Au[13] film (which was used as an electrode only) of the same thickness was deposited on a positively polarized plane. The catalyst is denoted here as (−)Ag.

The electric circuit for the generation of TERO was the same as that employed before. Briefly, an electric signal from a network analyzer (Anritsu MS3606B) was amplified (Kalmus, 250FC) and applied to a catalyst after impedance adjustment. The resonance frequencies of TERO appeared at 3.5, 10.5, 17.4, and 24.1 MHz in accordance with the frequencies calculated by a piezoelectric equation, and the primary resonance frequency of 3.5 MHz was used.

The catalytic ethanol decomposition was carried out in a gas-circulating vacuum apparatus, and reactants and products were analyzed by an on-line gas chromatograph. The measurements and precise control of the catalyst temperature were described elsewhere.[7]

Lattice displacement caused by TERO was measured by using a homemade laser Doppler apparatus. A (−)Ag catalyst was

10.1021/jp021166k CCC: $22.00
Published on Web 09/05/2002

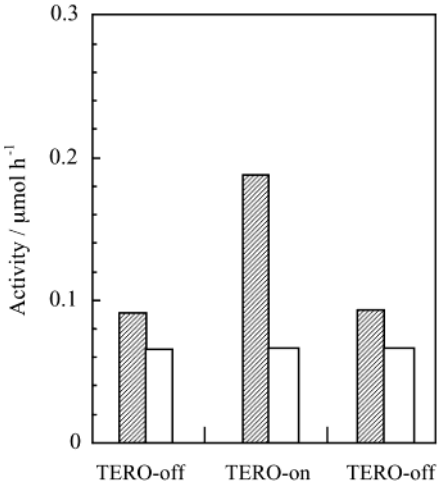

Figure 1. Changes in catalytic activity with TERO on and TERO off: (shaded bars) ethylene; (white bars) acetaldehyde. Reaction temperature, $T_r = 593$ K; rf power, $J = 3$ W; ethanol pressure, $P_e = 4.0$ kPa.

mounted on a stage movable for the x and y directions. The surface was irradiated by a He−Ne laser beam, and a reflected beam was monitored by a vibrometer (Ono sokki LV-1300).[7] Lattice displacement was shown as three-dimensional $x-y-z$ images.

Photoelectron emission spectra were obtained in air by a low-energy photoelectron spectroscopic method.[12] A (−)Ag surface was irradiated with monochromatized UV light from a deuterium lamp. The wavelength of light was scanned over the range of 230−300 nm, and the numbers of emitted electrons were counted against photon energy. The threshold energy for photoelectron emission was measured in the absence and presence of TERO, and the emission spectra were compared with those previously obtained for (+)Ag.

Results

Figure 1 shows changes in the catalytic activity for ethanol decomposition with TERO on and TERO off. The (−)Ag catalysts provided slightly larger amounts of ethylene than those of acetaldehyde in gas phase. With turning on rf power to generate the TERO, an immediate increase in ethylene production occurred, but no significant enhancement was observed with acetaldehyde production. With TERO off, the activity for ethylene production returned to nearly the same level as that before TERO on.

Figure 2 shows the temperature dependences of the reaction rate over the temperature range 573−653 K. Without TERO, the slope of linear relationship yielded an activation energy of 156 kJ mol^{-1} for ethylene production and 95 kJ mol^{-1} for acetaldehyde production. With TERO on, the temperature dependence for ethylene production became slightly smaller, and the activation energy decreased to 146 kJ mol^{-1}. No changes in temperature dependence of acetaldehyde production occurred, and the activation energy remained unchanged. A fall of the activation energy with TERO on was considerably smaller for (−)Ag, compared to a decrease to 103 kJ mol^{-1} for (+)Ag.[13]

Figure 3 shows the pressure dependence of ethanol decomposition on (−)Ag. In the absence of TERO, no significant changes in the reaction rate with ethanol pressure were observed for both ethylene and acetaldehyde productions, which was indicative of zero order with respect to ethanol pressure, P_e. With TERO on at 3 W, little changes in the pressure dependence were observed, and the reaction orders remained as zero order.

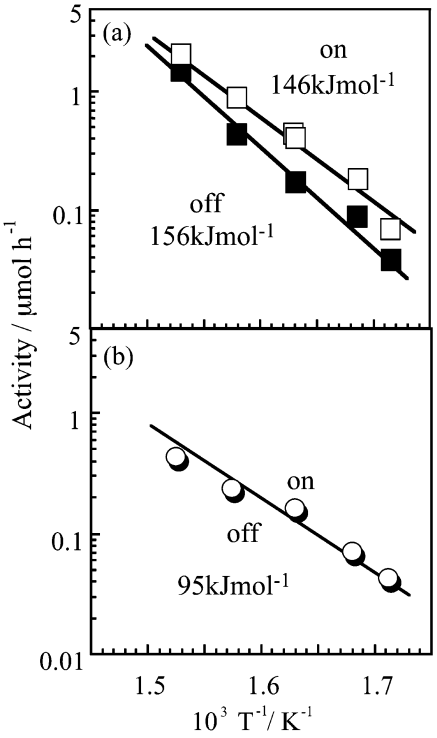

Figure 2. Temperature dependence of (a) ethylene and (b) acetaldehyde production in ethanol decomposition with (□, ○) TERO on and (■, ●) TERO off. $J = 3$ W; $P_e = 4.0$ kPa.

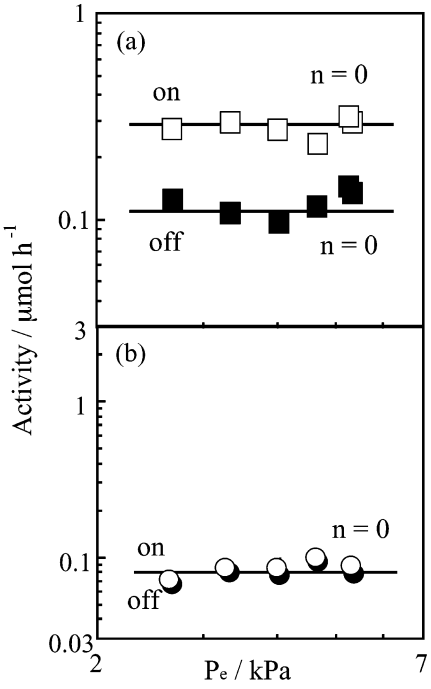

Figure 3. Pressure dependence of (a) ethylene and (b) acetaldehyde production with (□, ○) TERO on and (■, ●) TERO off. $T_r = 593$ K; $J = 3$ W.

Figure 4 shows the activities for ethylene and acetaldehyde production as a function of rf power. For comparison, the figure also shows the results previously obtained for (+)Ag.[13] The activity increased in a nonlinear manner with increasing power, but the activity enhancement of ethylene production was quite different between (−)Ag and (+)Ag: the increases were significantly smaller for (−)Ag than for (+)Ag. For the acetaldehyde production, even though the activity increases were

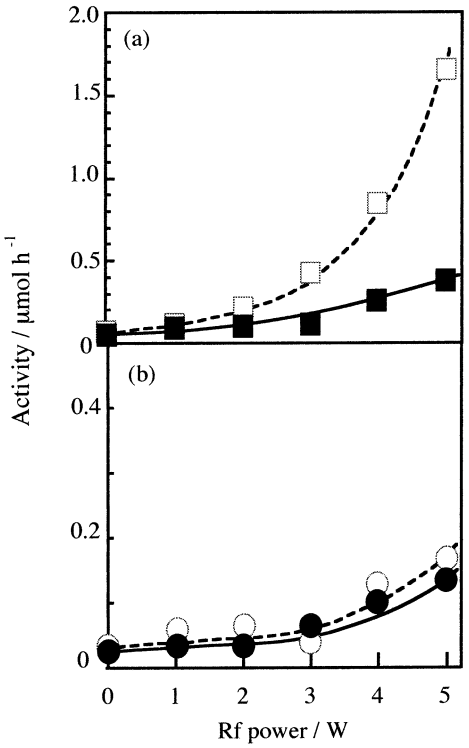

Figure 4. Catalytic activity for (a) ethylene and (b) acetaldehyde production as a function of rf power: (■, ●, solid lines) (−)Ag; (□, ○, dotted lines) (+)Ag (cf. ref 13). $T_r = 593$ K; $P_e = 4.0$ kPa.

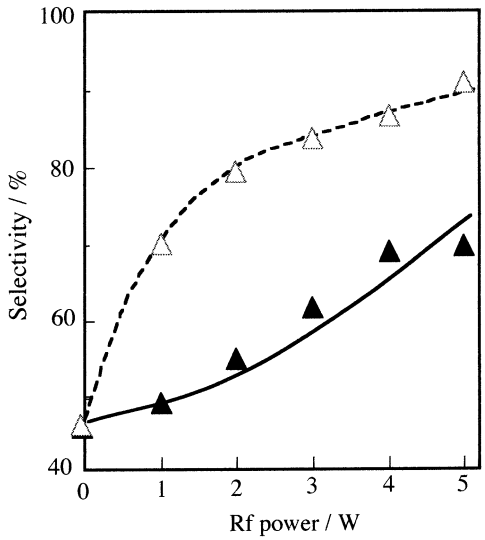

Figure 5. Selectivity for ethylene production as a function of rf power: (▲, solid line) (−)Ag; (△, dotted line) (+)Ag (cf. ref 13). $T_r = 593$ K; $P_e = 4.0$ kPa.

not large for both (−)Ag and (+)Ag, the TERO effects were slightly smaller for (−)Ag than for (+)Ag.[13]

Figure 5 shows changes in the selectivity for ethylene production with rf power. For (−)Ag, a selectivity of 44% without TERO increased gradually with increasing rf power and reached 70% at 5 W. The increase was significantly smaller compared to 91% for (+)Ag.

The X-ray diffraction pattern of a 100 nm thick (−)Ag provided two diffraction peaks at $2\theta = 38.2°$ and $2\theta = 44.4°$, assigned to the (111) and (200) plane, respectively. The diffraction peaks were the same as those observed for (+)Ag. The X-ray photoelectron spectra showed that the binding energy

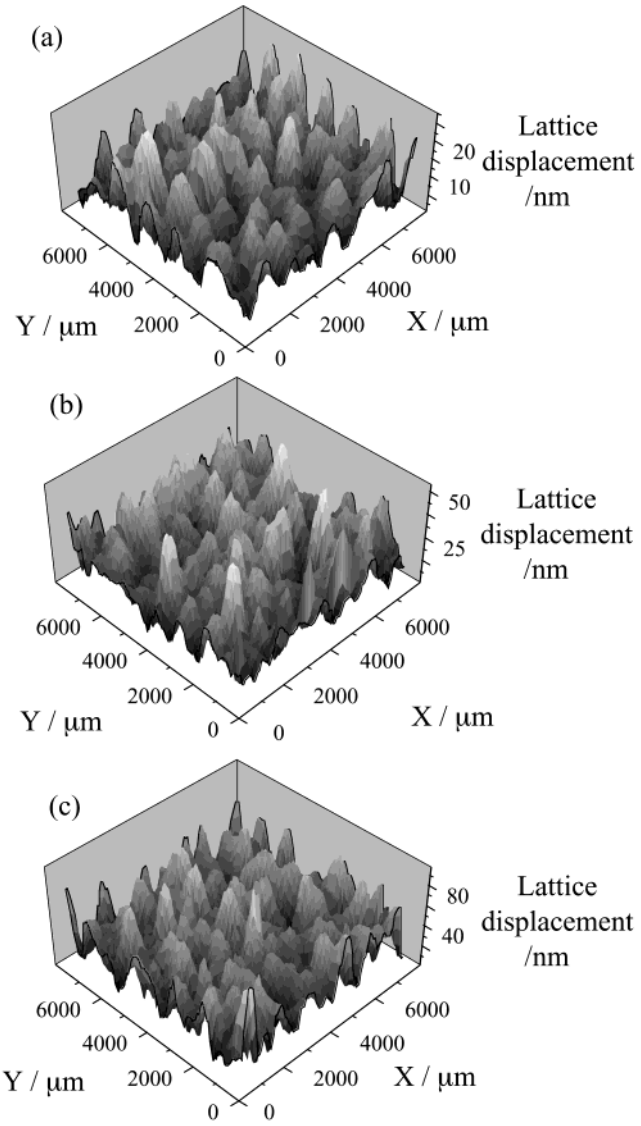

Figure 6. Three-dimensional laser Doppler images with TERO on: (a) $J = 1$ W; (b) $J = 3$ W; (c) $J = 5$ W. Temperature of measurements, T_m = room temperature.

of Ag $3d_{5/2}$ level of (−)Ag was 368.1 eV. This value was the same as that of (+)Ag.

Figure 6 shows three-dimensional laser Doppler patterns induced by the TERO. The patterns are composed of randomly distributed vertical standing waves over the $x-y$ directions. With increasing rf power, the standing waves grew significantly. The amplitude of the waves corresponded to lattice displacement. Figure 7 shows changes in the distribution of lattice displacements with rf power. The maximum lattice displacement, L_{max}, and the average lattice displacement, L_{av}, were 30 and 9 nm at 1 W, respectively. The full width at half-maximum (fwhm) was 7 nm. At 3 W, L_{max} and L_{av} increased to 56 and 18 nm, respectively. The fwhm was 18 nm. At 5 W, L_{max} was attained at 78 nm and L_{av} at 24 nm. The fwhm increased to 25 nm,.

Figure 8 shows photoelectron emission spectra from a (−)Ag surface with TERO off and TERO on. Photoelectron emission was observed at 4.45 eV in the absence of TERO. With TERO on at 3 W, the emission spectra moved toward larger photon energy, and electron emission occurred at 4.52 eV, indicating a shift of threshold energy by 0.07 eV. At 5 W, the threshold energy increased to 4.54 eV. Figure 9 shows the threshold energy, Φ, as a function of rf power, together with previous

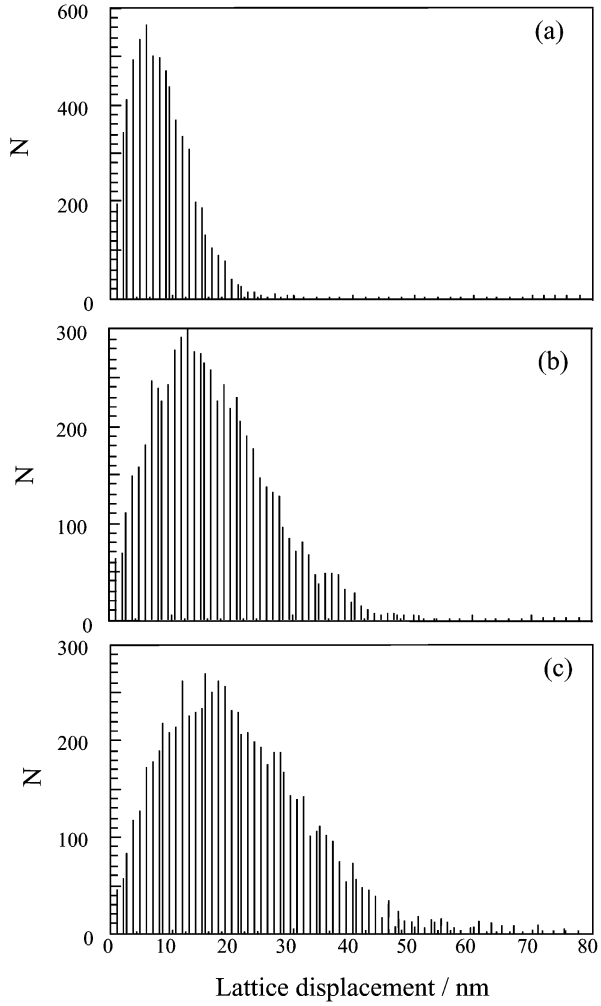

Figure 7. Distributions of lattice displacement with different power levels: (a) $J = 1$ W; (b) $J = 3$ W; (c) $J = 5$ W. T_m = room temperature.

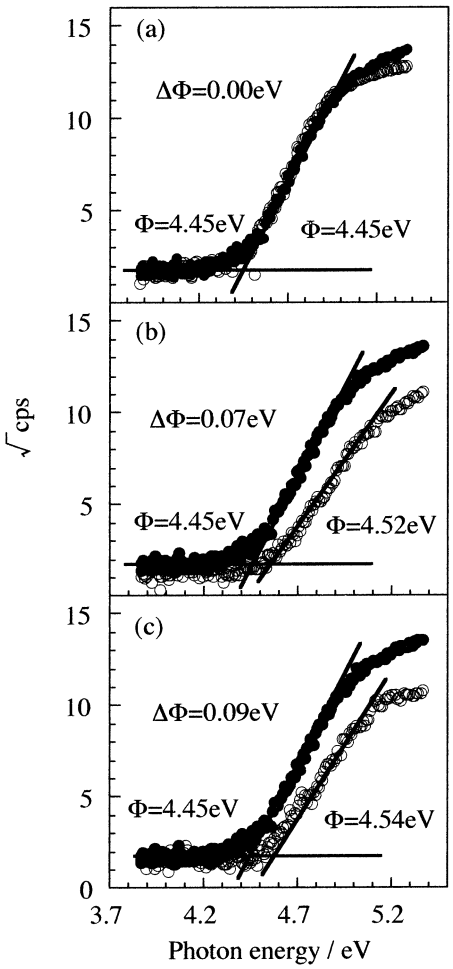

Figure 8. Photoelectron emission spectra of (−)Ag with (○) TERO on and (●) TERO off: (a) $J = 1$ W; (b) $J = 3$ W; (c) $J = 5$ W. T_m = room temperature.

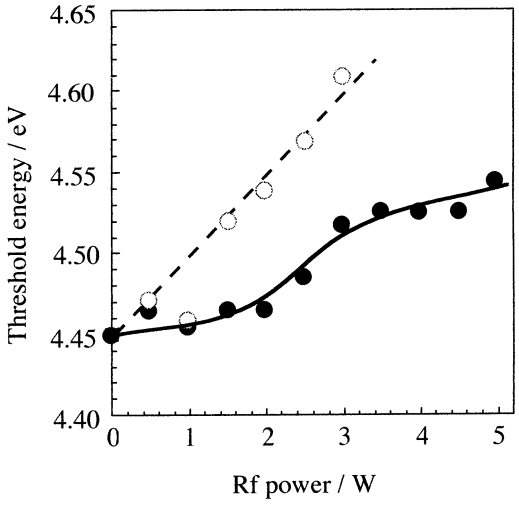

Figure 9. Threshold energy of Ag surfaces as a function of rf power: (●, solid lines) (−)Ag; (○, dotted line) (+)Ag (cf. ref 13).

results for (+)Ag.[13] The threshold energy of (−)Ag remained nearly unchanged up to 2 W and increased gradually with increasing power. The shift of 0.09 eV at 5 W was significantly smaller than 0.16 eV obtained at 3 W for (+)Ag.

Discussion

For ethanol decomposition on (−)Ag, the TERO gave rise to the selective activation of ethylene production without significant influences on the activity for acetaldehyde production. The feature was similar to that observed for (+)Ag.[13] However, the TERO effects on (−)Ag were significantly smaller, compared to those on (+)Ag. With TERO on, the activation energy of ethylene production decreased from 156 to 146 kJ mol^{-1} for (−)Ag, whereas it decreased to 103 kJ mol^{-1} for (+)Ag: the extent of activation energy decrease with the TERO was 6% for (−)Ag and 34% for (+)Ag. In a previous study of a Ag catalyst in which a thin Ag film was deposited on both the positive and negative polar planes of *z*-LN, TERO caused a decrease in the activation energy for ethylene production to 115 kJ mol^{-1}. It should be noted that this value was intermediate between (+)Ag and (−)Ag. The catalytic activity for ethylene production with TERO on at 5 W increased 4-fold for (−)Ag, but 15-fold for (+)Ag. Increases in the selectivity for ethylene production with increasing rf power were much smaller for (−)Ag than for (+)Ag: at 5 W, the selectivity was 70% for (−)Ag but more than 90% for (+)Ag. Thus, it is evident that the TERO effects were significantly larger for (+)Ag than for (−)Ag, indicating the presence of polarization-axis dependence in the TERO effects.

Irrespective of the absence and presence of TERO, the reaction order remained as zero. This order was the same as that obtained for the reaction on (+)Ag and can be derived by assuming that the rate-determining step is the decomposition of strongly adsorbed and fully surface-covering ethanol, as discussed previously for (+)Ag.[13]

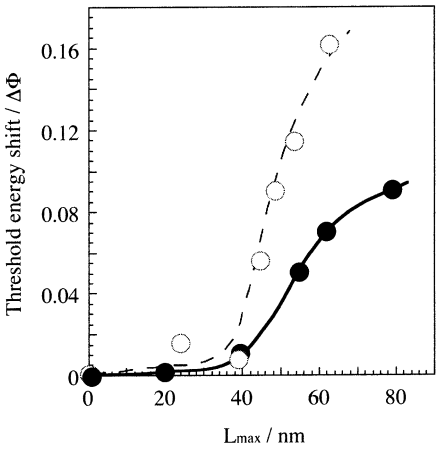

Figure 10. Correlations between threshold energy shift and maximum lattice displacement, L_{max}: (●, solid lines) (−)Ag; (○, dotted line) (+)Ag (cf. ref 13).

In laser Doppler measurements, the TERO for (−)Ag showed randomly distributed standing waves, indicating the generation of lattice displacement vertical to the surface. L_{max} and L_{av} changed in similar manner with increasing power between (−)Ag and (+)Ag. At 5 W, L_{max} and L_{av} of (−)Ag were 78 and 24 nm, respectively, which were similar to those of (+)Ag. Thus, it is evident that the lattice displacements were analogous between (−)Ag and (+)Ag, and a possibility can be ruled out that large differences in the TERO effects between (−)Ag and (+)Ag are due to a difference in lattice displacement caused by the TERO.

As shown in the photoelectron emission spectra, the TERO caused the threshold energy shift toward higher photon energy. Because the threshold energy is related to the work function, the results indicate that the work function increased in the presence of the TERO. It was shown that the work function shift was larger for (+)Ag than for (−)Ag at the same rf power. The differences between them can be seen more clearly when the work function shifts were compared with the lattice displacement. As shown in Figure 10, for the same lattice displacement, significantly larger work function shifts were observed for (+)Ag compared to those for (−)Ag. In a jellium model, the work function of a transition metal is mainly determined by a dipole electronic layer.[15,16] The layer is composed of the negative charges due to electrons that spill out from the topmost layer of the metal surface and of the positive charges remaining in the interior of the surface. To explain changes in the work function with the TERO, a model is proposed that the vertical lattice displacement has strong influences on the density of "spilled out" electrons. This assumption is based on the fact that the work function varies only when the direction of lattice displacement is consistent with the direction toward which electrons spill out, because the positive work function shift was invoked with the TERO of vertical lattice displacement but not induced with the TSRO of parallel lattice displacement. From these results, it is suggested that differences in the TERO effects on the catalytic activity between (−)Ag and (+)Ag are mainly associated with different changes in the work function.

Previous studies[8,9] of Pd and Ag deposited on the positively and negatively polarized planes of *z*-LN demonstrated that the TERO generated negative voltages for (+)Pd and (+)Ag and positive voltages for (−)Pd and (−)Ag. The generation of the opposite voltages with respect to the polarized surfaces indicates that the polarization axis controls the behavior of electrons: the polarization field accelerates electrons toward the positive polar surface and depresses electrons toward the negative polar surface. Thus, it is likely that the polarization direction has significant effects on the density of spilled-out electrons. A model for different TERO effects between (−)Ag and (+)Ag is shown in Figure 11. The polarization axis toward the (+) plane increases the density of spilled out electrons, whereas the polarization axis with the reverse direction works in an opposite way. This causes larger work function shifts for (+)Ag than for (−)Ag.

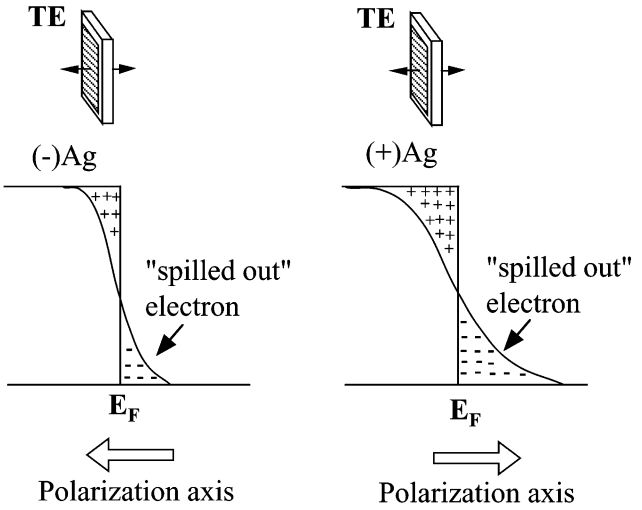

Figure 11. A model for the role of polarization axis direction in different work function shifts between (−)Ag and (+)Ag.

The TERO effects on the selective ethylene production are discussed in a previous study of (+)Ag. The proposed model was that the TERO caused an increase in the work function, leading to weak interactions between the adsorbed molecules and the Ag surfaces, because of lowering of Fermi level.[17,18] This converts an ethoxy species to a molecularly chemisorbed ethanol. The adsorption geometry of the latter has an advantage of easier abstraction of HOH groups, because the O−H bond was oriented parallel to the metal surface.[19] Thus, larger work function shifts lead to the higher activity and selectivity enhancements for ethylene production. This is in line with the observed results for (−)Ag and (+)Ag.

In conclusion, the TERO has polarization-dependent effects on catalyst activation. The different TERO effects are associated with different changes in work function-related electronic properties at the metal surface.

Acknowledgment. This work was supported by a Grant-in-Aid for Scientific Research (B) from The Ministry of Education, Science, Sports, and Culture.

References and Notes

(1) Inoue, Y. *Catal. Surv. Jpn.* **1999**, *3*, 95.
(2) Ohkawara, Y.; Saito, N.; Inoue, Y. *Surf. Sci*. **1996**, *357/358* (6), 777.
(3) Nishiyama, H.; Saito, N.; Shima, M.; Watanabe, Y.; Inoue, Y. *J. Chem. Soc. Faraday Discuss*. **1997**, *107*, 425.
(4) Saito, N.; Ohkawara, Y.; Watanabe, Y.; Inoue, Y. *Appl. Surf. Sci*. **1997**, *121/122*, 343.
(5) Ohkawara, Y.; Saito, N.; Inoue, Y. *Chem. Phys. Lett*. **1998**, *286*, 502.
(6) Saito, N.; Ohkawara, Y.; Sato, K.; Inoue, Y. *MRS Symp. Proc*. **1998**, *497*, 215.
(7) Saito, N.; Nishiyama, H.; Sato, K.; Inoue, Y. *Chem. Phys. Lett*. **1998**, *297*, 72.
(8) Saito, N.; Sato, K.; Inoue, Y. *Surf. Sci*. **1998**, *417*, 384.
(9) Saito, N.; Nishiyama, H.; Sato, K.; Inoue, Y. *Surf. Sci*. **2000**, *454/456*, 1099.

(10) Saito, N.; Nishiyama, H.; Inoue, Y. *Appl. Surf. Sci*. **2001**, *169/170*, 259.
(11) Ohkawara, Y.; Saito, N.; Inoue, Y. *Solid State Ionics* **2000**, *136/137*, 819.
(12) Saito, N.; Inoue, Y. *J. Chem. Phys*. **2000**, *113*, 469.
(13) Saito, N.; Inoue, Y. *J. Phys. Chem. B* **2002**, *106*, 5011.
(14) Yukawa. Y.; Saito, N.; Nishiyama, H.; Inoue, Y. *J. Phys. Chem. B*, in press.
(15) Lang, N. D.; Kohn, W. *Phys. Rev*. **1970**, *B1*, 4555.
(16) Smith, J. R. *Phys. Rev*. **1969**, 181, 522.
(17) Marcel, R. I. *Principles of Adsorption and Reactions on Solid Surfaces*; Wiley: New York, 1996.
(18) Somorjai, G. *Introduction to Surface Chemistry and Catalysis*; Wiley: New York, 1994.
(19) Kratochwil, Th.; Wittmann, M.; Küppers, J. *J. Electon Spectrosc. Relat. Phenom*. **1993**, *64/65*, 609.